Effective Enhancement of Anticorrosive Properties of Polystyrene by Polystyrene–Clay Nanocomposite Materials

Jui-Ming Yeh, Shir-Joe Liou, Chih-Guang Lin, Yen-Po Chang, Yuan-Hsiang Yu, Chi-Feng Cheng

Department of Chemistry and Center for Nanotechnology at CYCU, Chung-Yuan Christian University, Chung Li, Taiwan 320, ROC

Received 24 March 2003; accepted 20 June 2003

ABSTRACT: A series of polymer–clay nanocomposite (PCN) materials consisting of polystyrene (PS) and layered montmorillonite (MMT) clay was prepared by effectively dispersing the inorganic nanolayers of MMT clay in the organic PS matrix via *in situ* thermal polymerization. Organic styrene monomers were first intercalated into the interlayer regions of organophilic clay hosts, followed by a typical free radical polymerization with BPO as the initiator. The as-synthesized PCN materials were characterized by infrared spectroscopy (IR), wide-angle powder X-ray diffraction (XRD) and transmission electron microscopy (TEM). PCN coatings with low clay loading (1 wt %) on cold-rolled steel (CRS) were found to be superior in anticorrosion to those of bulk PS, based on a series of electrochemical measurements of corrosion potential, polarization resistance and corrosion current in a 5 wt % aqueous NaCl electrolyte. The molecular weights of PS extracted from PCN materials and bulk PS were determined by gel permeation chromatography (GPC) with tetrahydrofuran (THF) as the eluent. The effects of material composition on molecular barrier and thermal stability of PS and PCN materials, in the form of both free-standing films and fine powders, were also studied by molecular permeability analysis, differential scanning calorimetry (DSC) and thermogravimetric analysis (TGA), respectively. © 2004 Wiley Periodicals, Inc. J Appl Polym Sci 92: 1970–1976, 2004

Key words: polystyrene (PS); clay; nanocomposites

INTRODUCTION

Conventionally, polymeric coatings are used as a physical barrier on metallic surfaces to protect against attack by corrosive species (e.g. O_2 and H^+). However, polymeric coatings are not permanently impenetrable; once there are defects formed in the coatings, pathways will be created for the corrosive species to damage the metallic substrate, and localized corrosion will occur. Accordingly, many pigments with a lamellar or plate-like shape (e.g. micaceous iron oxide and aluminum flakes) have been introduced into polymeric coatings to effectively increase the length of diffusion pathways for oxygen and water as well as to decrease the permeability of the coating.[1] Montmorillonite (MMT), a material with a lamellar shape, has drawn considerable research attention in the preparation of polymer–clay nanocomposites (PCN) for novel, effective anticorrosion materials.

The chemical structure of MMT typically consists of two fused silica tetrahedral sheets sandwiching an edge-shared octahedral sheet of either magnesium or aluminum hydroxide. The Na^+ and Ca^{+2} ions residing in the interlayer regions can be replaced by organic cations, such as alkylammonium ions, by a cationic-exchange reaction to render the hydrophilic layer of silicate organophilic. The early development of PCN can be traced to the research on polyamide–clay nanocomposites reported by Toyota's group in 1990.[2] The dispersion of nanolayers of mineral clay in various polymer matrices has been reported to boost the thermal stability,[3] mechanical strength,[4] molecular barrier[5] and flame retardant[6] properties of polymers based on many recently published studies.

Polystyrene (PS) is one of the most popular and widely-used polymers. Many researchers are interested in studies of PS–clay hybrid nanocomposite materials.[7–15] Giannelis et al. report that the intercalation of PS into organophilic clay interlayers can be achieved by heating a mixture of PS and organophilic clay above the glass transition temperature of PS.[8] Lee et al. demonstrated the synthesis and characterization of PS–clay nanocomposites by emulsion polymerization.[9] Toyota Central Research group reported the preparation of PS–clay by melt blending a styrene vinyloxazoline copolymer with organophilic clay.[10]

Recently, we reported that dispersing nanolayers of mineral clay into polymer matrices enhances the corrosion inhibition of conjugated polyaniline[16] and nonconjugated poly(methyl methacrylate)[17] on metallic surfaces via the formation of PCN coatings, based on a series of electrochemical corrosion measurements of corrosion potential, polarization resistance and corrosion current.[8] However, the anticorrosive performance

Correspondence to: J.-M. Yeh (juiming@cycu.edu.tw).

Journal of Applied Polymer Science, Vol. 92, 1970–1976 (2004)

of PS–clay nanocomposite materials on metallic surfaces has never been reported.

Therefore, in this article, we present the first evaluation of the anticorrosive effects of nonconjugated PCN coatings, PS–clay. The as-synthesized PS–clay nanocomposite materials were characterized by wide-angle powder X-ray diffraction (XRD), transmission electron microscopy (TEM) and infrared (IR) spectroscopy. PCN materials in the form of coatings with low clay loading on cold-rolled steel (CRS) were found to be superior in anticorrosion to those of bulk PS, based on a series of electrochemical measurements of corrosion potential, polarization resistance and corrosion current in a 5 wt % aqueous NaCl electrolyte. Furthermore, we found that a further increase of clay loading resulted in a slightly enhanced molecular barrier property of PCN materials. The molecular weights of PS extracted from PCN materials and bulk PS were determined by gel permeation chromatography (GPC) with tetrahydrofuran (THF) as the eluent. The effects of material composition on the O_2/H_2O molecular barrier and thermal stability were also studied with molecular permeability analysis, differential scanning calorimetry (DSC) and thermogravimetric analysis (TGA), respectively.

EXPERIMENTAL

Chemicals and instrumentation

Polystyrene (M_w = 280,000) (Aldrich), styrene (Aldrich, 99%), benzoyl peroxide (Riedel-De Haen, 98%), 1-methylpyrrolidinone (Tedia, 99.6%), THF for GPC (Fisher Scientific, 99.8%), lithium chloride (Acros., 99%), hydrochloric acid (Riedel-De Haen, 37%), THF for reagent (Riedel-De Haen) and methanol (Riedel-De Haen) were used as received without further purification. Hexadecyltrimethylammonium chloride, $CH_3(CH_2)_{15}N^+(CH)_3Cl^-$ (Fluka, 98.0%), was used as an intercalating agent. The MMT clay, supplied by Pat-Kong Ceramic Company, had a unit cell formula of $[Na_{0.48}K_{0.01}Ca_{0.01}Ti_{0.01}](Fe_{0.20}Mg_{0.31}Al_{1.44})(Si_{3.93}Al_{0.07})O_{10}(OH)_2 \bullet ZH_2O$ and a CEC value of 98 mEq/100g.

Wide-angle XRD study of the samples was performed on a Rigaku D/MAX-3C OD-2988N X-ray diffractometer with a cooper target and a Ni filter at a scanning rate of 2°/min. The samples for TEM study were first prepared by putting powder of PCN materials into PS resin capsules and curing the PS resin at 100°C for 24 h in a vacuum oven. Then the cured PS resin containing PCN materials were microtomed with a Reichert-Jumg Ultracut-E into 60≈90 nm thick slices. Subsequently, one layer of carbon of about 10 nm in thickness was deposited on these slices on mesh 100 copper nets for TEM observations on a JEOL-200FX with an acceleration voltage of 120 KV. FTIR spectra were recorded on pressed KBr pellets using a BIO-RAD FTS-7 FTIR spectrometer. A Perkin–Elmer thermal analysis system equipped with model 7 DSC and model 7/DX TGA were employed for the thermal analyses under air flow. The programmed heating rate was 20°C/min in most cases.

Electrochemical measurements of corrosion potential, polarization resistance and corrosion current on sample-coated CRS coupons were performed with a VoltaLab 21 Potentiostat/Galvanostat in a standard corrosion cell equipped with two graphite rod counter-electrodes and a saturated calomel electrode (SCE) as well as the working electrode. The molecular weight of polymer extracted from all composite samples as well as bulk PS was determined with a Perkin–Elmer model TC4 equipped with a model 590 programmable solvent delivery module, a differential refractometer detector and a Styragel HT column with THF as the eluent and monodispersed polystyrenes as calibration standards. A Yanagimoto Co., Ltd gas permeability analyzer (model GTR 10) was employed to perform the permeation experiments of oxygen gas and water vapor.

Synthesis of polystyrene

A representative procedure to prepare PS is as follows: 10.415 g (0.100 mole) of styrene monomer, 0.242 g (0.500 mmole) of BPO, and 37 mL of dry THF were put in a 250 mL three-neck round-bottomed flask connected to a condenser, a thermometer and a nitrogen gas inlet/outlet. Nitrogen gas was bubbled into the flask throughout the reaction. Under magnetic stirring, the solution was heated to 85°C and maintained for 24 h. The reaction mixture solution was then poured into about 500 mL of methanol to precipitate the polymer. After filtration, the polymer was dissolved in 60 mL of dry THF and reprecipitated in 500 mL of methanol. The purification procedure was repeated twice, and the purified polymer was dried under vacuum at room temperature for 48 h. A quantity of 8.5 g of PS was obtained in ≈80% yield.

Preparation of organoplilic clay

The organophilic clay was prepared by a cationic-exchange reaction between the sodium cations of MMT clay and the quaternary alkylammonium cations of $(CH_3(CH_2)_{15}N^+(CH)_3Cl^-)$. The equation for calculating the amount of intercalating agent used for the cationic-exchange reaction is as follows:

$$98/100 \times 5\ \text{g(for clay)} \times 1.2 = (X/M_w\text{of intercalating agent}) \times 1 \times 1000$$

where X represents the amount of intercalating agent used, 98/100 represents the CEC value per 100 g of

MMT clay, 1.2 (>1) indicates that an excess amount of intercalating agent was used. For most preparations, 5 g of MMT clay with a CEC value of 98 mEq/100 g was stirred in 400 mL distilled water (beaker A) at room temperature overnight. A separate solution was prepared by mixing an excess of intercalating agent (1.91 g) with another 30 mL of distilled water (beaker B), under magnetic stirring, followed by adding 1.0*M* HCl aqueous solution to adjust the pH value to about 3-4. After stirring for 1 h, the protonated amino acid solution (beaker B) was added at a rate of approximately 10 mL/min with vigorous stirring to the MMT suspension (beaker A). The prepared mixture was then stirred overnight at room temperature. Organophilic clay was recovered by ultracentrifuging (9000 rpm, 30 min) and filtering the solution with a Buchner funnel. Purified products were obtained by sequential washing and filtering of the samples at least three times to remove any excess of ammonium ions.

Preparation of polystyrene–clay nanocomposite materials

Following a typical procedure for the preparation of PCN materials with 1 wt % clay loading, an appropriate amount of organophilic clay (0.1 g) was introduced into 100 mL of THF under magnetic stirring overnight at room temperature. A quantity of 9.9 g of styrene monomer was subsequently added to the solution, which was stirred for another 24 h. Upon the addition of benzoyl peroxide, the solution was stirred for 24 h at 85°C under a N_2 atmosphere. The synthesized lamellar nanocomposite precipitates were then obtained by precipitating from excess methanol (500 mL) and subsequent drying under dynamic vacuum at room temperature for 48 h.

Polymer recovery (extraction)

A reverse cationic-exchange reaction was employed to separate bound PS from the inorganic components in the nanocomposite. Following a typical extraction procedure, 2 g of fine powder of the synthesized PCN was dissolved in ≈100 mL of THF (beaker A). In another beaker, 10 mL of a stock solution of 1 wt % $LiCl_{(s)}$ in THF was prepared (beaker B). Both beakers were under vigorous magnetic stirring for 3≈4 hours at room temperature. After combining the contents of the two beakers, the mixture was stirred overnight followed by Soxhlet extraction at 80°C for 24 h. The extracted solution was then poured into excess methanol to precipitate the polymer. After filtration, the polymer was dried under vacuum at room temperature for 48 h. Molecular weights of both the extracted and the bulk PS were determined by gel permeation chromatography analyses with THF as the eluent.

Preparation of coatings and electrochemical measurements

The PS and PCN fine powders were dissolved in NMP to give 2 wt % solutions to improve the film formation. The solutions were cast dropwise onto the CRS coupons (1.0 × 1.0 cm) followed by drying in air for 24 h at 40°C to give coatings of ≈30 μm thick, as measured by digimatic micrometer (Mitutoyo). The coating ability of PCN on CRS is similar to that of bulk PS. The coated and uncoated coupons were then mounted to the working electrode so that only the coated side of the coupon was in direct contact with the electrolyte. The edges of the coupons were sealed with super-fast epoxy cement (SPAR®). All of the electrochemical measurements of corrosion potential, polarization resistance and corrosion current were performed on a VoltaLab model 21 Potentiostat/Galvanostat and repeated at least three times. The electrolyte was a NaCl (5 wt %) aqueous solution. The open circuit potential (OCP) at the equilibrium state of the system was recorded as the corrosion potential (E_{corr} in volts vs. SCE). The polarization resistance (R_p in °/cm^2) was measured by sweeping the applied potential from 20 mV below to 20 mV above the E_{corr} value at a scan rate of 500 mV/min and recording the corresponding current change. The R_p value was obtained from the slope of the potential-versus-current plot. The Tafel plots were obtained by scanning potential from 250 mV below to 250 mV above the E_{corr} value at a scan rate of 500 mV/min. The corrosion current (i_{corr}) was determined by superimposing a straight line along the linear portion of the cathodic or anodic curve and extrapolating it through E_{corr}. The corrosion rate (R_{corr}, in milli-inches per year, (MPY) was calculated using the following equation:

$$R_{corr}(\text{MPY}) = [0.13\ i_{corr}(\text{E.W.})]/[A \cdot d]$$

where E.W. is the equivalent weight (in g/Eq), A is the area (in cm^2) and d is the density (in g/cm^3).

Preparation of free-standing films and barrier property measurements

In order to enhance the mechanical strength of free-standing films of as-synthesized materials for molecular (H_2O and O_2) barrier property measurements under high pressure difference conditions, a commercial PS with high molecular weight (M_w = 280,000) was blended into the casting solution for film formation. Typically, 0.1 g of the as-synthesized PS or PCN materials blended with 0.1 g of commercialized PS was dissolved in 10 mL of NMP under magnetic stirring at room temperature for 4 h. The solution was cast onto a substrate (e.g. a microscope glass slide). The solvent was allowed to evaporate at 90≈100°C

TABLE I
Relations of Composition of PS–MMT Clay Nanocomposite Materials to E_{corr}, R_p, i_{corr} and R_{corr} Measured by Electrochemical Methods

Compound Code	Feed Composition (wt %)		Inorganic Content in Product[a] (wt %)	Electrochemical Corrosion Measurements*				Thickness[b] (μm)
	Polystyrene	MMT		E_{corr} (mV)	R_p (K$\Omega \cdot$ cm^2)	i_{corr} (nA/cm^2)	R_{corr} (MPY)	
Bare	—	—	—	−604	2.7	1.9×10^4	36.7	—
PS	100	0	0	−486	30.0	2.8×10^3	5.4	31
CLPS1	99	1	2.8	−450	96.0	4.5×10^2	8.7×10^{-1}	33
CLPS3	97	3	7.4	−429	1.9×10^2	2.5×10^2	4.8×10^{-1}	32
CLPS5	95	5	8.6	−417	4.4×10^2	1.8×10^2	3.5×10^{-1}	31
CLPS10	90	10	11.2	−329	6.1×10^2	1.4×10^2	2.7×10^{-1}	30

[a] As determined from TGA measurements.
[b] As measured by a digimatic micrometer.
* Saturated calomel electrode was employed as reference electrode.

under the hood for 24 h. The sample-coated glass substrate was then immersed in distilled water for 24 h to give a free-standing film of PS and PCN materials. Oxygen permeability values of free-standing films (called membranes) were determined by using the Yanco GTR-10 gas permeability analyzer. The gas permeability was calculated using the following equation:

$$P = l/(p_1 - p_2) \times \frac{q/t}{A}$$

where P is the gas permeability [cm^3(STP)-cm/cm^2-sec-cmHg], q/t is the volumetric flow rate of gas permeate [cm^3(STP)/sec], l is the free-standing film thickness [cm], A is the effective free-standing film area [cm^2] and p_1 and p_2 are the pressures (cmHg) on the high pressure and low pressure sides of the free-standing film, respectively. The rate of transmission of O_2 was obtained by gas chromatography, from which the air permeability was calculated. The study of water vapor permeation was carried out by using the same apparatus as that used for pervaporation, except that the feed solution was not in contact with the membrane.

RESULTS AND DISCUSSION

MMT is a clay mineral containing stacked silicate sheets measuring ≈10 Å in thickness and ≈2180 Å in length.[18] It possesses a high aspect ratio (about 220) and a plate-like morphology. MMT has a high swelling capacity, which is important for efficient intercalation of the polymer, and is composed of stacked silicate sheets that offer enhanced thermal stability, mechanical strength, flame retardance and molecular barrier properties.

To synthesize the PCN materials, organophilic clay was first prepared by a cation-exchange reaction between the sodium cations of MMT clay and the alkylammonium or alkylphosphonium ions of the intercalating agent. Organic MMA monomers were subsequently intercalated into the interlayer regions of organophilic clay hosts, followed by a typical free radical polymerization. The composition of the PCN materials was varied from 0 to 10 wt % of clay with respect to PS content, as summarized in Table I.

Characterization

Representative FTIR spectra of the organophilic clay, bulk PS and PCN materials are shown in Figure 1. The characteristic vibration bands of PS appear at 1450 cm^{-1}, 1500 cm^{-1} and 1600 cm^{-1} (aromatic C==C),

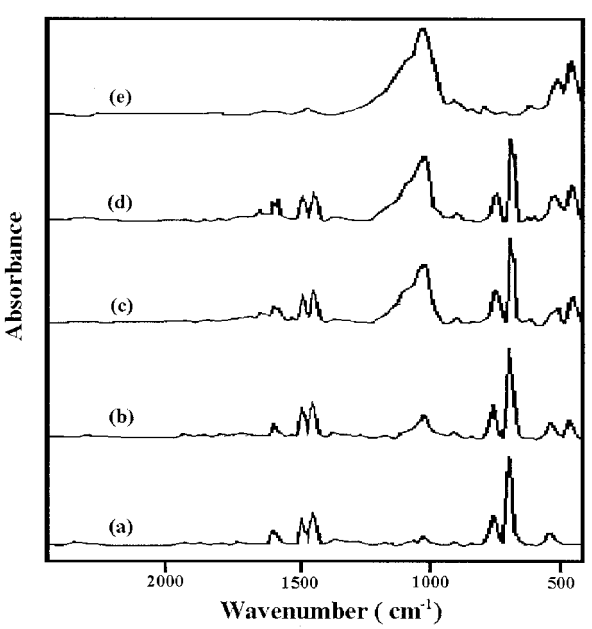

Figure 1 FTIR spectra of (a) clay, (b) CLPS1, (c) CLPS5, (d) CLPS10 and (e) organophilic clay.

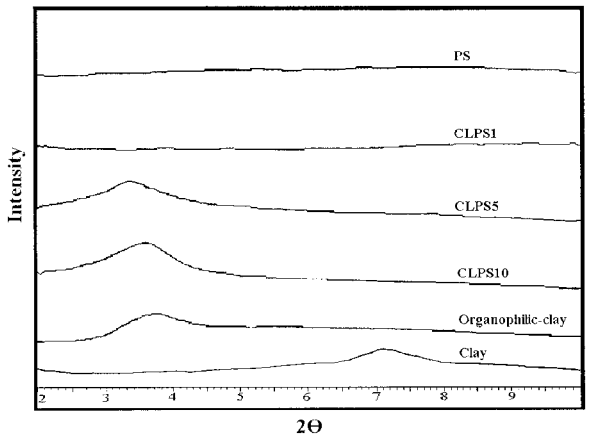

Figure 2 Wide-angle powder XRD patterns of organophilic clay, PS and a series of PS–clay nanocomposite materials.

and those of MMT clay are shown at 1040 cm^{-1} (Si—O), 600 cm^{-1} (Al—O) and 420 cm^{-1} (Mg—O).[19] As the loading of MMT clay increased, the intensities of MMT clay bands became stronger in the FTIR spectra of PCN materials. Figure 2 shows the wide-angle powder XRD patterns of organophilic clay and a series of PCN materials. For CLPS1, there is a lack of diffraction peak at 2θ = 2–10°, as opposed to the diffraction peak at 2θ = 3.75° (d spacing = 23.5 Å) for organophilic clay, indicating the possibility of exfoliated silicate nanolayers of organophilic clay dispersed in the PS matrix. When the amount of organoclay increased to 5%, a small peak appeared at 2θ = 3.40°, corresponding a d spacing of 26.3 Å. This implies that there is a small amount of organoclay that cannot be exfoliated in the PS and exists in the form of an intercalated layer structure. In Figure 3, the TEM of PCN materials with 5 wt % clay loading reveals that the nanocomposite displays a mixed nanomorphology. Individual silicate layers, along with two and three layer stacks, are found to be exfoliated in the PS matrix. In addition, some larger intercalated tactoids can also be identified.

M_w determination of extracted and bulk PS

Molecular weights and molecular weight distribution of the polymer samples recovered from the nanolayers of MMT clays were obtained by GPC analyses with THF as the eluent. All of the GPC elution patterns of the samples displayed a single peak, corresponding to a molecular weight value, as summarized in Table II. The PCN materials were found to exhibit an obvious decrease in molecular weight and a narrower molecular weight distribution (MWD) compared to Bulk PS, indicating the structurally restricted polymerization situations of styrene monomers in the intragallery region of the MMT clay[20] and/or the nature of clay–oligomer interactions, such as adsorption, during the polymerization reaction.

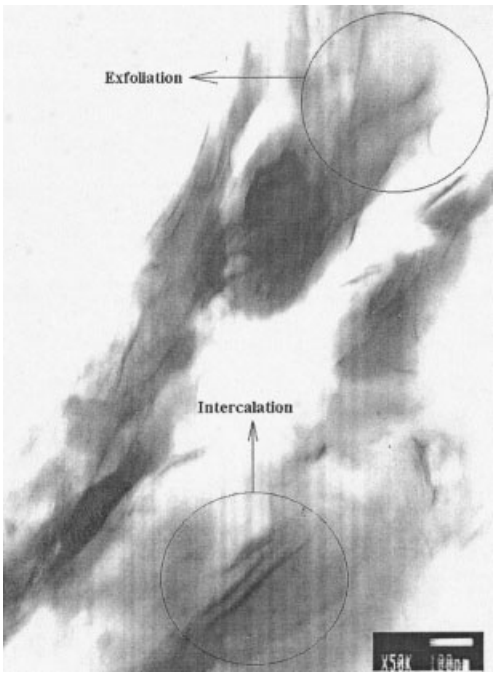

Figure 3 TEM of CLPS5.

Anticorrosion performance of coatings

Anticorrosive performance of sample-coated CRS coupons can be evaluated from the values of corrosion potential (E_{corr}), polarization resistance (R_p), corrosion current (i_{corr}) and corrosion rate (R_{corr}), as listed in Table I. The CRS coupon coated with PS showed a higher E_{corr} value than the uncoated CRS. However, it exhibited a lower E_{corr} value than the specimen coated with PCN materials. For example, the CLPS1-coated CRS had a high corrosion potential of about −450 mV at 30 min. Even after 5 h of measurement, the potential remained at about −460 mV. Such an E_{corr} value implies that the CLPS1-coated CRS is more noble towards the electrochemical corrosion than the PS. The CLPS1-coated CRS shows a polarization resistance (R_p) value of 9.6 = 10^1 k°/cm^2 in 5 wt % NaCl, which approaches 2 orders of magnitude greater than that of the uncoated CRS. The Tafel plots for uncoated, PS-

TABLE II
Molecular Weights of Bulk and Extracted PS

Sample	M_w	M_n	M_w/M_n
PS	44700	23500	1.90
CLPS1	42100	23900	1.76
CLPS3	37300	21200	1.75
CLPS5	23900	14500	1.65
CLPS10	2100	13100	1.60

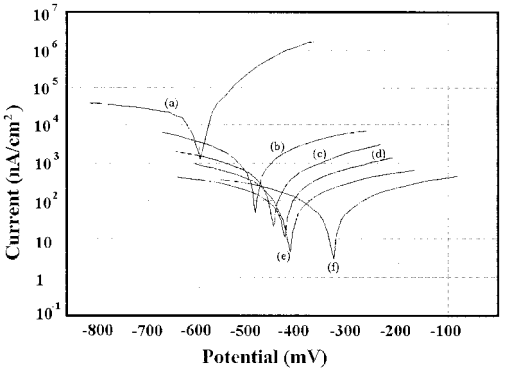

Figure 4 Tafel Plots for (a) uncoated, (b) PS-coated, (c) CLPS1-coated, (d) CLPS3-coated, (e) CLPS5-coated and (f) CLPS10-coated CRS measured in a 5 wt % NaCl aqueous solution.

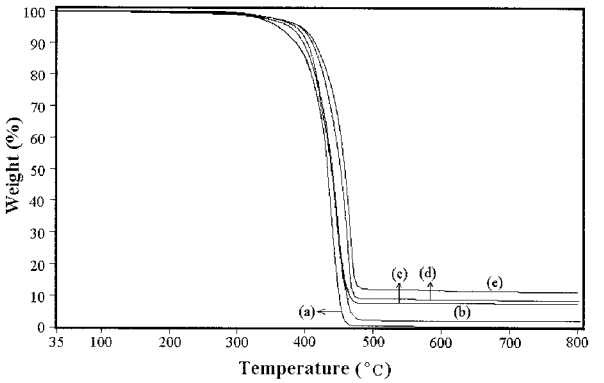

Figure 6 TGA curves of (a) PS, (b) CLPS1, (c) CLPS3, (d) CLPS5 and (e) CLPS10.

coated, CLPS1-coated, CLPS3-coated, CLPS5-coated and CLPS10-coated CRS are shown in Figure 4. For example, the corrosion current (i_{corr}) of CLPS1-coated CRS is approximately 4.5×10^2 nA/cm^2, which corresponds to a corrosion rate (R_{corr}) of about 8.7×10^{-1} MPY (Table I). Electrochemical corrosion current values of PCN materials as coatings on CRS were found to decrease gradually with increasing clay loading. This novel property of enhanced anticorrosion effect for PS–clay nanocomposite materials compared to bulk PS may arise from dispersing silicate nanolayers of clay in the PS matrix to increase the tortousity of the diffusion pathway of oxygen and water. This is further evidenced by the studies of the O_2 and H_2O molecular barrier effect, as discussed in the following section.

Molecular barrier properties of free-standing films

In this study, the free-standing films (called membranes) of PCN materials and bulk PS used for the molecular barrier measurements were prepared to have a film thickness of ≈30 μm. Compared to PS, free-standing films of PCN materials at low clay loading (1 wt %) show about 57% and 15% decrease in H_2O and O_2 permeability, respectively, as shown in Figure 5. Furthermore, it should be noted that a further increase in clay loading results in a slightly enhanced molecular barrier property of bulk PCN materials.

Thermal properties of fine powders

Figure 6 shows typical TGA thermograms of weight loss as a function of temperature for the PS and PCN materials, as measured under an air atmosphere. In general, there appear to be several stages of weight loss starting at ≈300°C and ending at 800°C, which may correspond to the degradation of intercalating agent followed by the structural decomposition of the polymers. Evidently, the thermal decomposition of the PCN materials shifts toward higher temperatures than that of PS, which confirms the enhancement of thermal stability of intercalated PS.[7] DSC traces of the Pure PS and PCN materials are shown in Figure 7. The pure PS exhibits an endotherm at 86.5°C, corresponding to the T_g of PS.[15] All of the PCN materials show an increased T_g compared to pure PS. This is tentatively attributed to the confinement of the intercalated polymer chains

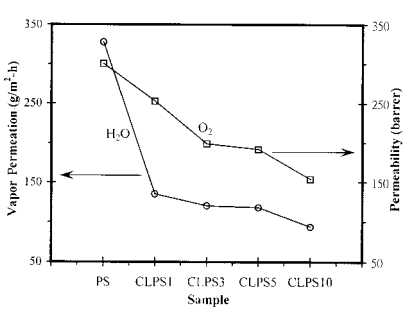

Figure 5 Permeability of H_2O and O_2 as a function of MMT clay content in the PS–clay nanocomposite materials.

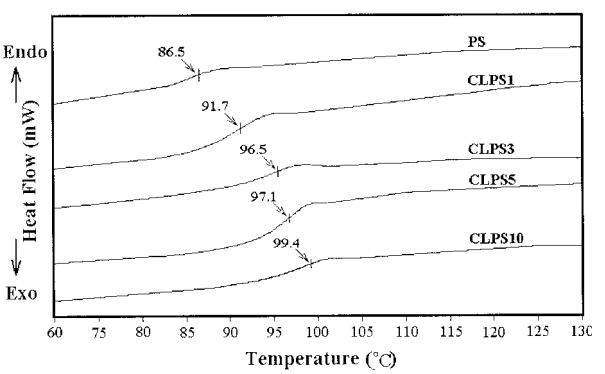

Figure 7 DSC curves of PS and a series of PS–clay nanocomposite materials.

within the clay galleries that prevents the segmental motions of the polymer chains.

CONCLUSIONS

A series of PCN materials was prepared by effectively dispersing the inorganic nanolayers of MMT clay in an organic PS matrix via *in situ* thermal polymerization. Organic styrene monomers were first intercalated into the interlayer regions of organophilic clay hosts, followed by a typical free radical polymerization. The as-synthesized PCN materials were characterized by IR spectroscopy, wide-angle powder XRD and TEM. PCN coatings with low clay loading (1 wt %) on CRS were found to be superior in anticorrosion to those of bulk PS, based on a series of electrochemical measurements of corrosion potential, polarization resistance and corrosion current in a 5 wt % aqueous NaCl electrolyte. Enhanced anticorrosion of PS–clay nanocomposite materials compared to bulk PS may result from dispersing silicate nanolayers of clay in the PS matrix to increase the tortousity of the diffusion pathway of oxygen and water. The molecular weights of PS extracted from PCN materials and bulk PS were determined by GPC with THF as the eluent. The molecular weights of extracted PS were found to be slightly lower than that of the bulk PS, indicating the structurally restricted polymerization situations in the intragallery region of the MMT clay and/or the nature of clay–oligomer interactions, such as adsorption, during the polymerization reaction. The effects of material composition on the molecular barrier and thermal stability of PS and PCN materials, in the form of both free-standing films and fine powders, were also studied by molecular permeability analysis, DSC and TGA. The free-standing films (called membrane) of PCN materials at low clay loading (1 wt %) showed about 57% and 15% reduction of H_2O and O_2 permeability, respectively, compared to PS. Thermal decomposition of those PCN materials shifts toward the higher temperature range than that of PS based on the TGA studies, which confirms the enhancement of thermal stability of intercalated PS. All of the PCN materials showed an increased T_g compared to pure PS based on the DSC studies. This is tentatively attributed to the confinement of the intercalated polymer chains within the clay galleries that prevents the segmental motions of the polymer chains.

The financial support of this research by the NSC 90-2113-M-033-010 is gratefully acknowledged.

References

1. Li, P.; Tan, T. C.; Lee, J.Y. Synth Met 1997, 88, 237.
2. Usuki, A.; Kaisumi, M.; Kojima, Y.; Okada, A.; Karauchi, T., Kamigaito, O. J Mater Res 1993, 8, 1774.
3. Lan, T.; Kaviratna, P. D.; Pinnavaia, T. J. Chem Mater 1994, 6, 573.
4. Tyan, H.-L.; Liu, Y.-C.; Wei, K.-H. Chem Mater 1999, 11,1942.
5. Wang, Z.; Pinnavaia, T. J. Chem Mater 1998, 10, 3769.
6. Gilman, J. W.; Jackson, C. L.; Morgan, A. B.; Hayyis, R., Jr.; Manias, E.; Giannelis, E. P.; Wuthenow, M.; Hilton, D.; Phillips, S. H. Chem Mater 2000, 12, 1866.
7. Fu, X.; Qutubuddin, S. Polymer 2001, 42, 807.
8. Vaia, R. A.; Jandt, K. D.; Kramer, E. J.; Giannelis, E. P. Chem Mater 1996, 8, 2628.
9. Noh, M.-W.; Lee, D. C. Polym Bull 1999, 42, 619.
10. Hasegawa, N.; Okamoto, H.; Kaisumi, M.; Usuki, A. J Appl Polym Sci 1999, 74, 3359.
11. Zax, D. B.; Yang, D.-K.; Santos, R. A.; Hegemann, H. J. Chem Phys 2000, 112, 6, 2945.
12. Vaia, R. A.; Ishii, H.; Giannelis, E. P. Chem Mater 1993, 5, 12, 1695.
13. Krishnamoorti, R.; Vaia, R. A.; Giannelis, E. P. Chem Mater 1996, 8, 1728.
14. Doh, J. G.; Cho, I. Polym Bull 1998, 41, 511.
15. Sikka, M.; Cerini, L. N.; Ghosh, S. S.; Winey, K. I. J Polym Sci: Part B: Polym Phys 1996, 34, 1443.
16. Yeh, J.-M.; Liou, S.-J.; Lai, C.-Y.; Wu, P.-C.; Tsai, T.-Y. Chem Mater 2001, 13, 1131.
17. Yeh, J.-M.; Liou, S.-J.; Lin, C.-Y.; Cheng, C.-Y.; Chang, Y.-W.; Lee, K.-R. Chem Mater 2002, 14, 1, 154.
18. Yano, K.; Usuki, A.; Okada, A. J Polym Sci, Polym Chem Ed 1997, 35, 2289.
19. Kim, J. W.; Choi, H. J.; Jhon, M. S. Macromol Symp 2000, 155, 229.
20. Wrobleski, D. A.; Benicewicz, B. C.; Thompson, K. G.; Byran, C. J. Polym Prepr (Am Chem Soc, Div Polym Chem) 1994, 35(1), 265.